Chemical Physics 75 (1983) 425–441
North-Holland Publishing Company



# CLUSTER EXPANSION OF THE WAVEFUNCTION. VALENCE AND RYDBERG EXCITATIONS, IONIZATIONS, AND INNER-VALENCE IONIZATIONS OF $CO_2$ AND $N_2O$ STUDIED BY THE SAC AND SAC CI THEORIES

Hiroshi NAKATSUJI

*Department of Hydrocarbon Chemistry, Faculty of Engineering, Kyoto University, Kyoto 606, Japan*

Received 13 September 1982

Valence and Rydberg excitations, ionizations, and inner-valence ionizations of $CO_2$ and $N_2O$, which are isoelectronic, are studied by the SAC and SAC CI theories. We have given a systematic assignment of the electronic spectra of these molecules, though there were some controversial situations in the assignment of the spectra. The broad and overlapping features of the spectra of the inner-valence ionizations are due to the existence of a large number of ionization–excitation states mixing with the singly ionized states. The theoretical origins of the similarities and differences in the photoelectron spectra of $CO_2$ and $N_2O$ are clarified.

## 1. Introduction

Studies of electron correlations of molecules in open-shell and excited states are current topics in theoretical quantum chemistry. Several approaches are being developed, multi-reference (MR) CI [1], MC SCF [2], and cluster expansion [3]. In this series of papers, we are developing cluster expansion theories, called SAC (symmetry-adapted-cluster) theory [4,5] and SAC CI theory [6,7], for the studies of electron correlations in ground and various excited states of molecules. The excited states so far studied are singlet and triplet excited states, ionized states, and electron attached states, which are all essentially one-electron excited states [8], and the shake-up states involved in the inner-valence ionization [9], which are essentially two-electron excited states. The theories have also given a basis for deriving an orbital theory, called pseudo-orbital theory [4], for studies of spin correlations in open-shell radicals [10]. Recently, spin correlations, electron correlations and their couplings in doublet radicals have been studied by the SAC and SAC CI theories [11].

Here, we study the ground and several vertical excited states of $CO_2$ and $N_2O$, isoelectronic molecules. We are interested in the electronic excitations (valence and Rydberg), valence ionizations, and inner-valence ionizations. For $CO_2$, there are some controversial situations in the assignments of the excitation spectra [12–20]. England and Ermler gave a good review for this situation [12–15]. Earlier CI calculations with modest expansions [16] seemed to explain well the experimental spectra observed in those days [19]. However, later more elaborate CI calculations gave very different results [12–15], except for the equation-of-motion calculations by England et al. [20]. The fact that the valence excited states of $CO_2$ should be strongly bent [21] seems to make an analysis of the spectra rather complicated [12]. A similar situation may be expected for the spectra of $N_2O$ [22,23]. It is interesting to study systematically the valence and Rydberg excitations of $CO_2$ and $N_2O$.

The ionization spectra of $CO_2$ and $N_2O$ are also of interest. They are observed from valence to inner-valence regions by photoelectron spectroscopy [24–26] and by dipole (e–2e) spectroscopy [27,28]. In the valence region, the lowest ionization potential of $CO_2$ seems to be rather difficult to be reproduced accurately by the CI method [12]. In the inner-valence region, the experimental spectra of $CO_2$ and $N_2O$ are very broad and overlapping, suggesting an existence of many satellite peaks. Cederbaum et al. [29] and Domcke et al. [28] studied these spectra theoretically by the 2ph TDA Green's function technique [30] and attributed the origin of these spectra as being due to a complete breakdown of the Hartree–Fock model in this region of the spectra. The present SAC CI theory was applied previously to the inner-valence ionizations of water and the results were satisfactory [9]. Here, we apply the theory to $CO_2$ and $N_2O$.

In section 2, we briefly summarize the theoretical background of the present study and the calculational details. In section 3, we give the results for the ground and excited states of $CO_2$ and $N_2O$. We study valence and Rydberg excitations and give systematic assignments of the spectra, some of which are different from the previous ones [17–19,22,23]. In section 4, we study the ionization spectra of $CO_2$ and $N_2O$. We study both outer- and inner-valence ionizations and their satellite peaks. These spectra show some interesting complexity caused by a complete breakdown of the Hartree–Fock model. They include simultaneous ionization–excitation (shake-up) processes. A summary and conclusions of the present study are given in section 5.

## 2. Theoretical background and calculational details

Theories of the SAC [4,5] and SAC CI [6,7] expansions have been given previously in detail. Here, we give a brief account pertinent to the present study. We describe the ground states of $CO_2$ and $N_2O$ by the SAC expansion,

$$\Psi_g = \exp\Big(\sum_I C_I S_I^\dagger\Big)|0\rangle, \tag{1}$$

where $S_I^\dagger$ is a symmetry-adapted excitation operator and $|0\rangle$ is a Hartree–Fock reference configuration. This expansion includes self-consistency [31] and multiple effects of correlations [32]. The variational principle leads to the formula,

$$\langle\Psi_g|(H-E_g)S_I^\dagger|\Psi_g\rangle = 0, \tag{2}$$

which is a generalized Brillouin theorem. Requiring the Schrödinger equation within the space of the linked configurations $|0\rangle$ and $S_I^\dagger|0\rangle$, we obtain the non-variational (NV) solution

$$\langle 0|(H-E_g)|\Psi_g\rangle = 0, \quad \langle 0|S_I(H-E_g)|\Psi_g\rangle = 0. \tag{3}$$

The excited states and ionized states, including both valence and inner-valence ionizations, of $CO_2$ and $N_2O$ are studied by the SAC CI theory. Though these states can also be studied directly by the SAC theory [5,11], the use of the SAC CI theory is more efficient and convenient [33]. In the SAC CI theory, we first define the excited functions $\{\Phi_K\}$ as

$$\Phi_K = \mathscr{P} R_K^\dagger \Psi_g, \tag{4}$$

where $\mathscr{P}$ is a projector $\mathscr{P} = 1 - |\Psi_g\rangle\langle\Psi_g|$ which projects out the ground-state component, $R_K^\dagger$ is an excitation or ionization operator depending on whether we are dealing with excited states or ionized states, respectively, and $\Psi_g$ is the SAC wavefunction defined by eq. (1). Note that for singlet $A_1$ excited states, $R_K^\dagger$ in eq. (4) and $S_I^\dagger$ in eq. (1) denote in principle the same set of singlet $A_1$ symmetry-adapted excitation operators. We see then from eq. (2) that the excited functions $\{\Phi_K\}$ satisfy the following relations,

$$\langle\Phi_K|\Psi_g\rangle = 0, \tag{5a}$$

$$\langle\Phi_K|H|\Psi_g\rangle = 0. \tag{5b}$$

Namely, the functions $\{\Phi_K\}$ satisfy the necessary conditions for the excited-state wavefunctions [34]. The SAC equation (2) determines the ground state $\Psi_g$ *and at the same time* a set of the functions $\{\Phi_K\}$ as a basis for the excited states. Therefore, we describe the excited states $\Psi_e$ by linear combinations of the excited functions $\{\Phi_K\}$,

$$\Psi_e = \sum_K d_K \Phi_K, \tag{6}$$

which we call the SAC CI expansion. The SAC CI wavefunctions $\Psi_e$ satisfy automatically the orthogonality and the hamiltonian-orthogonality with the ground state (from eqs. (5a) and (5b), respectively), and also the similar relations with different excited states [7]. We note that when the ground state $\Psi_g$ is a solution of the NV equation (3), the above argument is not strictly valid. However, so long as the cluster expansion is accurate enough, the difference between the variational and non-variational solutions should be small. The variational solution of eq. (6) leads to the secular equation

$$\sum_L \langle \Phi_K | H - E_e | \Phi_L \rangle d_L = 0 \quad (7)$$

and the non-variational solution, as in eq. (3), leads to

$$\sum_L \langle 0 | R_K (H - E_e) | \Phi_L \rangle d_L = 0. \quad (8)$$

The non-variational solution includes the diagonalization of a large non-symmetric matrix. We have extended Davidson's algorithm for a symmetric matrix [35] to the non-symmetric case [36].

The SAC CI expansion is more rapidly convergent than an ordinary CI expansion [6–8] because it is based on the excited functions $\{\Phi_K\}$ which satisfy the necessary conditions for excited states, and because it starts from the ground-state correlation as seen from eq. (4). The spirit of multi-reference CI [1], i.e. correlation calculations starting from important multi-reference configurations, is included in the SAC CI theory through the unlinked terms (see eq. (12) below).

In actual calculations, some approximations are inevitable. The calculational scheme is the same as reported previously [8]. In the present calculation, we further adopted configuration selection [9,37]. The SAC expansion (1) was terminated up to second order

$$\Psi_g \approx \Big( 1 + \sum_I C_I S_I^\dagger + \tfrac{1}{2} \sum_{IJ} C_I C_J S_I^\dagger S_J^\dagger \Big) |0\rangle, \quad (9)$$

though this is done automatically in the NV calculation. For the linked operator $S_I^\dagger$, we have included all single-excitation operators

$$S_i^a = 2^{-1/2} \big( a_{a\alpha}^\dagger a_{i\alpha} + a_{a\beta}^\dagger a_{i\beta} \big) \quad (10)$$

and selected double-excitation operators, $S_i^a S_j^b$. ($i,j,k,l$ denote occupied MOs and $a,b,c,d$ unoccupied MOs.) We have included all double excitations whose contributions to the second-order perturbation energy with the HF reference $|0\rangle$ are larger than a given threshold $\lambda_g$

$$E_s = |H_{0s}|^2 / (H_{ss} - H_{00}) > \lambda_g, \quad (11)$$

where $\phi_s = S_i^a S_j^b |0\rangle$, $H_{0s} = \langle 0 | H | \phi_s \rangle$, $H_{ss} = \langle \phi_s | H | \phi_s \rangle$, and $H_{00} = \langle 0 | H | 0 \rangle$. In the unlinked terms, $\Sigma C_I C_J S_I^\dagger S_J^\dagger |0\rangle$, we have included only such double-excitation operators which have coefficients larger than $1 \times 10^{-2}$ in an ordinary CI including only linked terms. The unlinked term then includes only quadruple excitations $S_i^a S_j^b S_k^c S_l^d$.

In the SAC CI calculation, we have truncated eq. (6) as

$$\Psi_e = \Big( \sum_K d_K R_K^\dagger + \sum_{KI} d_K C_I R_K^\dagger S_I^\dagger \Big) |0\rangle - \sum_K d_K \mathbb{S}_{Kg} \Psi_g, \quad (12)$$

where $\mathbb{S}_{Kg} = \langle \Psi_g | R_K^\dagger \Psi_g \rangle$. The single- and double-excitation operators for the singlet and triplet excited states, ionized states, and electron attached states are summarized in table 1. As linked operators we have included these single- and double-excitation operators. Single-excitation operators were included without selection. Double-excitation operators were selected in the following way. Let $\Psi^{(p)}$ be a primary configuration

$$\Psi^{(p)} = \sum_i \alpha_i^{(p)} \phi_i^{(p)} \quad (p = 1, \ldots, N), \quad (13)$$

which is the sum of single-excitation or -ionization configurations $\phi_i^{(p)}$. $N$ is the number of states under consideration. We denote the doubly excited configuration to be selected as $\phi_s$ and define

$$\Delta E_{si}^{(p)} = |H_{si}^{(p)}|^2 / \big( H_{ii}^{(p)} - H_{ss} \big), \quad (14)$$

where $H_{si}^{(p)} = \langle \phi_s | H | \phi_i^{(p)} \rangle$, $H_{ii}^{(p)} = \langle \phi_i^{(p)} | H | \phi_i^{(p)} \rangle$, and $H_{ss} = \langle \phi_s | H | \phi_s \rangle$. We have included only such $\phi_s$ which satisfy

$$|\Delta E_{si}^{(p)}| > \lambda_e, \quad (15)$$

with at least one of the configurations $\phi_i^{(p)}$. As the configuration $\phi_i^{(p)}$ in eq. (13) we have included all single-excitation configurations which have coefficients larger than 0.1 in an ordinary single-excitation CI. In the unlinked term $\Sigma d_K C_I R_K^\dagger S_I^\dagger |0\rangle$, we have included all double-excitation operators $S_I^\dagger$

Table 1
Single- and double-excitation operators for singlet and triplet excitations, ionizations, and electron attachment [a)]

| Type of excitation | Single-excitation operator | Double-excitation operator |
|---|---|---|
| singlet excitation | $S_i^a = 2^{-1/2}(a_{a\alpha}^\dagger a_{i\alpha} + a_{a\beta}^\dagger a_{i\beta})$ | $S_i^a S_j^b$ |
| triplet excitation | $T_i^a = a_{a\alpha}^\dagger a_{i\beta}$ | $T_i^a S_j^b$ |
| ionization | $I_i = a_{i\beta}$ | $I_i S_j^a$ |
| electron attachment | $A^a = a_{a\alpha}^\dagger$ | $A^a S_i^b$ |

[a)] $i$, $j$ and $a$, $b$ denote occupied and unoccupied orbitals, respectively, in the reference Hartree–Fock configuration.

whose coefficients in the ground-state CI are larger than $1 \times 10^{-3}$. As for the $R_K^\dagger$ operator in the unlinked term, we did two types of selections. For singlet and triplet excitations and outer-valence ionizations, which are primarily single-electron processes, we have included only single-excitation operators whose coefficients in the CI including only linked operators are larger than 0.1. The unlinked term then includes triple excitations. For calculations of inner-valence ionizations and its satellites, which involve two-electron (simultaneous ionization–excitation) processes, we have included single- *and* double-excitation operators whose coefficients in the CI including only linked operators are larger than 0.1 [9]. The unlinked term then includes in this case triple and quadruple excitations. Hereafter, we refer to the calculations including only three-electron excited configurations and three- and four-electron excited configurations in the unlinked terms as "3-excited" and "3,4-excited" calculations, respectively.

Thus, the role of the *unlinked* terms in the SAC CI theory represents a spirit of the multi-reference CI; double excitations from important reference configurations. The coefficients of the double excitations are transferred from the SAC calculation for the ground state (cluster approximation). They are already involved in the $\Psi_g$ when we form the excited functions $\Phi_K$ by eq. (4). The reference configurations are singly excited configurations for the one-electron processes and doubly excited configurations for the two-electron processes. A sufficient number of reference configurations is selected automatically in our scheme because it does not result in an increase of the dimension of the matrix to be diagonalized. The size of the matrix to be diagonalized is determined by the number of *linked* terms.

We have used three kinds of basis set. They are a valence-only basis, a valence plus Rydberg basis, and a valence plus polarization basis. The valence-only bases of $CO_2$ and $N_2O$ are the (9s6p) GTOs of Huzinaga [38] contracted to the [3s2p] set by Dunning and Hay [39]. The valence plus Rydberg basis for $CO_2$ includes the [3s2p] set plus Rydberg 3s3p GTOs on each carbon and oxygen. For $N_2O$, the valence plus Rydberg set includes the [3s2p] set plus Rydberg 3s3p GTOs on only the central nitrogen. The Rydberg bases used are those given by Dunning and Hay [39]. The valence plus polarization basis includes the [3s2p] set plus d-polarization functions on each atom [39]. This basis was used for the calculations of the ground and ionized states of $CO_2$, since as von Niessen et al. pointed out [40], d-orbitals are important for the valence ionization potentials of $CO_2$. Though d-orbitals may also be important for the excitation energies [12–15], we did not test this possibility in the present calculation. The geometries of $CO_2$ and $N_2O$ were fixed at the experimental ones [41], C–O = 1.1621 Å for $CO_2$ and N–N = 1.1282 Å, N–O = 1.1842 Å for $N_2O$.

The values of the thresholds $\lambda_g$ and $\lambda_e$ in eqs. (11) and (15), respectively, are $1.0 \times 10^{-5}$ au and $5.0 \times 10^{-5}$ au for the calculations on $CO_2$ with all kinds of basis set and on $N_2O$ with the valence-only basis. For calculations on $N_2O$ with the valence plus Rydberg basis, we used the values $\lambda_g = 5.0 \times 10^{-5}$ au and $\lambda_e = 1.0 \times 10^{-4}$ au because of the lower symmetry of $N_2O$. Table 2 summarizes the dimensions of the matrices to be diagonalized in the present SAC and SAC CI calculations; i.e. the dimensions of the linked operators. The dimensions are rather small, considering the accuracy of the results shown below.

Table 2
Dimensions of the linked operators in the SAC and SAC CI calculations of $CO_2$ and $N_2O$ [a)]

| Molecule | State [b)] | Valence-only basis | | | Valence plus Rydberg basis [c)] | | |
|---|---|---|---|---|---|---|---|
| | | SE | DE | total | SE | DE | total |
| $CO_2$ | ground | 64 | 886 | 951 | 112 | 1231 | 1344 |
| | | | | | (136) | (2673) | (2810) |
| | excited singlet | | | | | | |
| | s | 64 | 437 | 501 | 112 | 1096 | 1208 |
| | a | 64 | 874 | 938 | 112 | 2316 | 2428 |
| | excited triplet | | | | | | |
| | s | – | – | – | 112 | 2860 | 2972 |
| | a | 64 | 1008 | 1072 | 112 | 1971 | 2083 |
| | ionized | | | | | | |
| | s | 4 | 311 | 315 | 4 | 426 | 430 |
| | | | | | (4) | (504) | (508) |
| | a | 4 | 314 | 318 | 4 | 449 | 453 |
| | | | | | (4) | (518) | (522) |
| $N_2O$ | ground | 128 | 1354 | 1483 | 160 | 904 | 1065 |
| | excited singlet | 128 | 1222 | 1350 | 160 | 2228 | 2388 |
| | excited triplet | 128 | 1325 | 1453 | 160 | 2457 | 2617 |
| | ionized | 8 | 578 | 586 | 8 | 682 | 690 |

[a)] SE: single excitation, DE: double excitation.
[b)] s and a denote symmetric and antisymmetric with respect to the $C_2$ operation.
[c)] Values in parentheses are for the valence plus polarization basis.

## 3. Ground states and valence and Rydberg excited states of $CO_2$ and $N_2O$

### 3.1. $CO_2$

The energy of the Hartree–Fock wavefunction used as a reference configuration and the correlation energy of the ground state of $CO_2$ are given in table 3. The orbital sequence of the Hartree–Fock configuration was calculated to be

$$(\text{core})^6\ 3\sigma_g^2\ 2\sigma_u^2\ 4\sigma_g^2\ 3\sigma_u^2\ 1\pi_u^4\ 1\pi_g^4. \tag{16}$$

The separation between the $3\sigma_u$ and $1\pi_u$ MOs was as small as 0.01 eV in the valence-only basis but became 0.70 eV in the valence plus polarization-basis (see table 8 below). For the correlation energy, the present results, even the single and double CI results, (1 + 2)CI, are lower than the previous results of Winter, Bender and Goddard [16] (WBG) and England and Ermler [12] (EE). The polarization function is very important: the SCF energy is lowered by 0.12 au and the correlation energy by 0.11 au. The total effect is as large as $-0.23$ au. The effect of the unlinked term is $\approx -0.02$ au. The effect of the Rydberg basis is very small, as expected, on the ground-state energy.

Table 4 shows the lower valence and Rydberg excitation energies of $CO_2$. All the excitations are vertical and are from the $1\pi_g$ and $1\pi_u$ MOs in an orbital picture. The Rydberg states are denoted by (R), though the mixing of the Rydberg and valence characters depends on the geometry [42], for example, the OCO angle [12–15]. The geometries of the excited states, which have the valence character of $1\pi_g \to 4\pi_u$, will be bent [21,41]. SECI denotes the results of the single-excitation CI. The results of WBG are parallel with the results of the SECI method. This probably reflects the smallness of the amount of the correlation effects included in the calculations of WBG. For valence excitations, the results of EE and ours are relatively similar but are very different from those of WBG

Table 3
Hartree–Fock energy and correlation energy of the ground state of $CO_2$ (au)

| Method | Present [a] | | | WBG [16] CI | EE [12] MC CI |
|---|---|---|---|---|---|
| | valence-only | valence plus Rydberg | valence plus polarization | | |
| Hartree–Fock [b] | −187.55292 | −187.55521 | −187.67466 | −187.5561 | −187.7226 |
| (1+2)CI [c] | −0.28670 | −0.28401 | −0.39869 | −0.1307 | −0.2570 |
| SAC NV | −0.30844 | −0.30317 | −0.41457 | | |

[a] Valence-only basis; [3s2p] CGTO of Dunning–Hay. Valence plus Rydberg basis; [3s2p] CGTO + Rydberg sp set on C and O. Valence plus polarization functions; [3s2p] CGTO + d-polarization functions on C and O.
[b] Hartree–Fock configuration is given in eq. (16).
[c] (1+2)CI denotes a CI including linked single and double excitations.

and of the SECI method. For Rydberg excitations, the results by WBG, EE, and us are rather similar. Especially, we note that the ordering of the states is the same in the SECI and WBG calculations and in the EE and the present calculations. The orderings between these two sets of calculations are different. Between the EE and the present results, the EE results are consistently higher than ours mostly by 0.1–0.2 eV. For the $^3\Sigma_u^+$ state, the EE value is higher than ours by 0.5 eV.

Between the results of WBG and the results of EE and ours, the largest difference is the location of the Rydberg $^{1,3}\Pi_g(R)$ states relative to the other valence states. In the WBG result, the $^{1,3}\Pi_g(R)$ states are well above the valence excited states of the $1\pi_g \to 4\pi_u$ character, but in the EE and our results, the $^{1,3}\Pi_g(R)$ states are embedded in the region of these valence excited states. From table 4, we see that by the addition of the Rydberg basis, the excitations of primarily valence character are shifted up by 0.07–0.14 eV. Further, we found a small mixing of valence excitations in the $^{1,3}\Pi_g(R)$ states.

The $^1\Delta_u$ and $^1\Pi_g(R)$ states are spectroscopically important [12], but the relative locations were not definitive in both experimental and theoretical studies [12]. The $^1\Sigma_u^-$ state has the same main electron configuration ($1\pi_g \to 4\pi_u$) as the $^1\Delta_u$ state. The present result is that the $^1\Pi_g(R)$ state, which is mainly of Rydberg nature, is lower than the $^1\Delta_u$ and $^1\Sigma_u^-$ states, which are valence in nature, at the vertically excited states. This supports the result of EE [12]. Due to England et al. [13], the SCF energy levels of the $^1\Delta_u$ and $^1\Pi_g$ states are essentially degenerate, so that the ordering and the spacing of these states are due to electron correlation. Table 4 shows that at the SECI level, the ordering of these states is reverse to the EE and the present fully correlated results. The same is true for the results of WBG [16]. Note that the Rydberg $^1\Pi_g(R)$ state has some small valence character and that the $^1\Pi_g(R)$, $^1\Delta_u$ and $^1\Sigma_u^-$ states mix strongly when the OCO angle is bent. As England and Ermler [12] discussed, an avoided crossing occurs between these states when the OCO angle is bent from 180°, and after the avoided crossing, the lower states become of valence character in contrast to the vertical excited states. The same situations occur also for the triplet counterparts, the $^3\Delta_u$ and $^3\Pi_g(R)$ states. Though the $^3\Pi_g(R)$ state is lower than the $^3\Delta_u$ state at the vertical excited states, they will mix strongly when the OCO angle is bent. An avoided crossing will soon occur and after that, the lower state will become of valence character.

The assignment of the experimental spectra [17–19] is not necessarily a straightforward task because they seem to be affected by the change in geometry, especially the OCO angle, in the excited states. When the geometry of the excited state differs from that in the ground state, the spectra develop to the lower-energy region. Ordinarily, the geometry of the Rydberg excited states should be linear in contrast to the bent geometry of the

Table 4
Lower valence and Rydberg vertical excitation energies of $CO_2$ (eV)

| State [a] | Orbital picture [b] | SECI | WBG [16] CI | EE [12] MC CI | SAC CI [c] | | Exptl. [12,16–19] |
|---|---|---|---|---|---|---|---|
| | | | | | valence only | valence plus Rydberg | |
| $^3\Sigma_u^+$ | $1\pi_g \to 4\pi_u$ | 7.24 | 7.35 | 8.65 | 8.04 | 8.15 | 8.1 |
| $^3\Pi_g$(R) | $1\pi_g \to 5\sigma_g(s)$ | 9.31 | 8.95 | 8.86 | – | 8.73 | 8.3 |
| $^3\Delta_u$ | $1\pi_g \to 4\pi_u$ | 8.02 | 7.83 | 9.02 | 8.67 | 8.80 | 8.8 |
| $^1\Pi_g$(R) | $1\pi_g \to 5\sigma_g(s)$ | 9.83 | 9.23 | 9.10 | – | 8.93 | 8.4–8.6 |
| $^3\Sigma_u^-$ | $1\pi_g \to 4\pi_u$ | 8.66 | 8.24 | 9.42 | 9.05 | 9.19 | |
| $^1\Sigma_u^-$ | $1\pi_g \to 4\pi_u$ | 8.66 | 8.27 | 9.42 | 9.13 | 9.27 | |
| $^1\Delta_u$ | $1\pi_g \to 4\pi_u$ | 8.99 | 8.38 | 9.43 | 9.25 | 9.32 | 9.3–9.4 |
| $^1\Sigma_u^+$(R) | $1\pi_g \to 2\pi_u(p_\pi)$ | 12.19 | 11.07 | 11.20 | – | 11.00 | 11.08–11.20 |
| $^3\Pi_u$(R) | $1\pi_g \to 4\sigma_u(p_\sigma)$ | 12.28 | 11.49 | 11.43 | – | 11.31 | |
| $^1\Pi_u$(R) | $1\pi_g \to 4\sigma_u(p_\sigma)$ | 12.46 | 11.53 | 11.45 | – | 11.39 | 11.4–11.6 |
| $^3\Sigma_g^+$ | $1\pi_u \to 4\pi_u$ | 11.04 | | 12.13 [d] | | 11.79 | |
| $^3\Delta_g$ | $1\pi_u \to 4\pi_u$ | 12.22 | | 12.91 [d] | | 12.44 | 12.4 |

[a] (R) denotes Rydberg excited state.
[b] In the calculations by the valence plus Rydberg basis, the $2\pi_u$, $3\pi_u$, and $4\pi_u$ MOs are mainly Rydberg orbital on C, Rydberg orbital on C and O, and valence $\pi$-antibonding orbital, respectively.
[c] SAC CI V solutions are given.
[d] Ref. [13].

valence excited states [21]. For the $^{1,3}\Pi_g$(R) states, however, the potential curves will become lower upon bending because of strong mixing (after the avoided crossing) with the $^{1,3}\Delta_u$ states [12]. Therefore, for the $^3\Sigma_u^+$, $^{1,3}\Pi_g$(R), and $^{1,3}\Sigma_u^-$ states, the theoretical values should be higher than the observed ones, but for the $^{1,3}\Delta_u$, $^1\Sigma_u^+$(R) and $^{1,3}\Pi_u$(R) states, the theoretical values should be close to experiment, so long as the theory is reliable. We then assign the peaks at $\approx 8.8$ eV, 9.3–9.4 eV, 11.08–11.20 eV, and 11.4–11.6 eV to the $^3\Delta_u$, $^1\Delta_u$, $^1\Sigma_u^+$(R), and $^1\Pi_u$(R) states, respectively. The optical peak at 8.4–8.6 eV, a counterpart of the optical peak at 9.3–9.4 eV, is then assigned to the $^1\Pi_g$(R) state. The peaks observed at $\approx 8.3$ eV and $\approx 8.1$ eV by electron impact spectroscopy [19] are assigned to the $^3\Pi_g$(R) and $^3\Sigma_u^+$ states, respectively. For the excitations from the inner $1\pi_u$ orbital, we have calculated only two triplet excited states. These are valence excitations of $1\pi_u \to 4\pi_u$ character, and will follow the first Rydberg band. The peak observed at 12.4 eV by electron impact spectroscopy [18] may be due to the $^3\Delta_g$ state. Though the present assignments do not necessarily agree with the assignments given by experimentalists [17–19], we have taken into accounts their arguments on the spectral intensities, especially the spin and space symmetries of the excited states.

### 3.2. $N_2O$

Table 5 shows the Hartree–Fock energy and the correlation energy of $N_2O$. The Hartree–Fock orbitals are calculated to be

$$(\mathrm{core})^6(4\sigma)^2(5\sigma)^2(6\sigma)^2(1\pi)^4(7\sigma)^2(2\pi)^4. \quad (17)$$

The present correlation energy is much lower than those of Peyerimhoff and Buenker [43] and of Winter [44]. (Winter's basis set is the same as the present valence-only basis.) This shows that the present wavefunction is much better than those of the earlier calculations. Between the present two results, the result of the valence plus Rydberg basis is worse because we have used a larger threshold $\lambda_g$ in eq. (11) for this basis than for the valence-only basis.

Table 5
Hartree–Fock energy and correlation energy of the ground state of NNO (au)

| Method | Present [a] | | Peyerimhoff and Buenker [43] | Winter [44] ($\Pi$ CI) |
|---|---|---|---|---|
| | valence only | valence plus Rydberg | | |
| Hartree–Fock [b] | −183.59033 | −183.59192 | −183.5763 | −183.59032 |
| (1+2)CI | −0.30634 | −0.28710 | −0.1108 | −0.12329 |
| SAC NV | −0.32688 | −0.30439 | | |

[a] The threshold for the linked operators in the SAC calculation, $\lambda_g$ in eq. (11), is $1.0 \times 10^{-5}$ au for the valence-only basis, but $5.0 \times 10^{-5}$ au for the valence plus Rydberg basis.
[b] Hartree–Fock configuration is given in eq. (17).

The dipole moment of $N_2O$ is sensitive to correlation effects. Table 6 shows the dipole moment and the second moment of $N_2O$. The SCF result of McLean and Yoshimine [45], which is near the Hartree–Fock limit, and the results of Peyerimhoff and Buenker [43] are cited for comparison. The SCF result of the dipole moment is much reduced by the inclusion of the correlation effect. The present CI result is smaller than that of Peyerimhoff and Buenker, reflecting the inclusion of a larger amount of correlation in the present calculation. The present SAC result is still smaller than the CI result with an increased inclusion of the correlation effect. It is less than a half of the SCF result. This reduction in dipole moment is due to a flow of charge from oxygen to the central nitrogen atom. The effects of electron correlation to the second moments are relatively small, but they work to bring the theoretical results closer to experiment. In the present case, the SAC results are closer to experiment than the CI results. In table 6, the SCF results of McLean and Yoshimine are closest to the experimental values. This shows the necessity of using a more extended basis set.

Table 7 shows the vertical excitation energies of $N_2O$. The Rydberg excited state is denoted by (R) in the first column. The CI results of Winter [44] and Peyerimhoff and Buenker [43] are cited for comparison. For Rydberg excitations, the present results seem to be the first calculations of fully correlated wavefunctions. For $N_2O$, the valence excitations of $2\pi \to 4\pi$ character appear separately as a group in a lower-energy region than the Rydberg excitations. For valence excitations, the present results are larger by 0.1–0.4 eV than the experimental values, probably because the geome-

Table 6
Dipole moment and second moment of the ground state of $N_2O$ (au)

| Property [a] | SCF limit [45] | PB [43] | | Present [b] | | | Exptl. [45] |
|---|---|---|---|---|---|---|---|
| | | SCF | CI | SCF | (1+2)CI [c] | SAC | |
| $\mu$ | – | −0.411 | −0.256 | −0.392 | −0.199 | −0.189 | ±0.653 |
| $\langle z^2 \rangle$ | 85.696 | 87.570 | 87.358 | 87.356 | 87.158 | 87.124 | 84.718 |
| $\langle x^2 \rangle + \langle y^2 \rangle$ | 22.898 | 22.986 | 23.086 | 23.048 | 23.048 | 23.042 | 22.793 |
| $\langle r^2 \rangle$ | 108.594 | 110.556 | 110.444 | 110.404 | 110.206 | 110.166 | 107.551 |

[a] The second moments were calculated with respect to the center of mass.
[b] Results of valence plus Rydberg basis.
[c] Single- and double-excitation CI including only linked configurations of the present SAC calculation.

Table 7
Lower valence and Rydberg vertical excitation energies of $N_2O$ (eV)

| State [a] | Orbital picture [b] | SECI [c] | W [44] $\Pi$ CI | PB [43] CI | SAC CI [d] valence only | SAC CI [d] valence plus Rydberg | Exptl. [44] |
|---|---|---|---|---|---|---|---|
| $^3\Sigma^+$ | $2\pi \rightarrow 4\pi$ | 4.23 | 5.4 | 5.8 | 5.76 | 5.75 | 5.6 |
| $^3\Delta$ | $2\pi \rightarrow 4\pi$ | 5.11 | 6.0 | 6.4 | 6.63 | 6.61 | 6.2 |
| $^3\Sigma^-$ | $2\pi \rightarrow 4\pi$ | 5.86 | 6.5 | 6.8 | 7.09 | 7.09 | |
| $^1\Sigma^-$ | $2\pi \rightarrow 4\pi$ | 5.86 | 6.6 | 6.9 | 7.26 | 7.16 | 6.81 [e], 6.85 |
| $^1\Delta$ | $2\pi \rightarrow 4\pi$ | 6.34 | 6.8 | 7.1 | 7.47 | 7.38 | |
| $^3\Pi$(R) | $2\pi \rightarrow 8\sigma(3s)$ | 8.45 | – | – | – | 8.38 | $\approx 8.0$ [f] |
| $^1\Pi$(R) | $2\pi \rightarrow 8\sigma(3s)$ | 8.99 | – | – | – | 8.60 | 8.52 |
| $^1\Sigma^+$(R) | $2\pi \rightarrow 3\pi(3p_\pi)$ | 10.56 | – | – | – | 9.84 | 9.66 |
| $^1\Delta$(R) | $2\pi \rightarrow 3\pi(3p_\pi)$ | 10.79 | – | – | – | 10.24 | |
| $^1\Sigma^-$(R) | $2\pi \rightarrow 3\pi(3p_\pi)$ | 10.84 | – | – | – | 10.27 | |

[a] (R) denotes Rydberg excited state.
[b] In the calculations by the valence plus Rydberg basis, the $3\pi$ and $4\pi$ MOs are mainly Rydberg and valence orbitals, respectively.
[c] Results of valence plus Rydberg basis. The results of valence only basis differ at most by 0.02 eV.
[d] Results of SAC CI V calculations.
[e] Ref. [17].
[f] Refs. [22,23].

tries of the excited states, especially the NNO angle, are different from that of the ground state; the geometry of the valence excited states should be bent [21]. For Rydberg excitations, the change in geometry due to the excitation should be small [21], so that the present SAC CI results for them agree better with the experimental values than for the valence excitations. The situation is simpler for $N_2O$ than for $CO_2$ because the avoided crossing between valence and Rydberg states does not occur for $N_2O$ because the latter are located in a higher-energy region than the former.

Comparing the results of the valence-only basis with those of the valence plus Rydberg basis, we see that the mixing of the valence and Rydberg characters is larger in the singlet states than in the triplet states. For the triplet states, the results of the two basis sets are almost the same. The mixing of valence and Rydberg characters in the singlet states occurs through electron correlation, since the SECI results of the two basis sets differed at most by only 0.02 eV.

The results of the SECI, $\Pi$ CI by Winter [44], and the limited CI by Peyerimhoff and Buenker [43] are all smaller than the present SAC CI results. The values increase in this order. The assignments of the two lowest peaks observed at 5.6 and 6.2 eV are the same, but for the peak at 6.85 eV, the assignments are different. Peyerimhoff et al. assigned it to either $^1\Sigma^-$ or $^3\Sigma^-$ and Winter assigned it to the $^1\Delta$ state. According to Rabalais et al. [17], who assigned this peak to the $^1\Delta$ state, this transition is of low intensity in optical spectra and the upper state involves considerable bond stretching and/or bending. Considering this fact and the results of the present SAC CI calculations, we prefer to assign this peak to the $^1\Sigma^-$ state, though the possibility of the $^1\Delta$ state still remains. The origin of the weak and broad peak seems to be due to a considerable bending in the excited state. For the Rydberg excitations, the present assignments are consistent with those of previous authors [17–19,22,44]. According to Hall et al. [22], the peak at $\approx 8.0$ eV is due to a spin-forbidden excitation and was assigned to the $^3\Pi$ state. Rabalais et al. [17] assigned the transitions at 8.52 and 9.66 eV to the $^1\Pi$ and $^1\Sigma^+$ states, respectively. The present results support these assignments.

## 4. Ionization spectra of $CO_2$ and $N_2O$ from outer- to inner-valence regions

### 4.1. Outer-valence ionization

Table 8 shows the ionization potentials of $CO_2$. The first four are outer-valence ionizations and the last two inner-valence ionizations. The latter two are the main peaks of many inner-valence ionizations and their satellites, which will be discussed in detail in section 4.2. The Koopmans values are always larger than the observed values. Von Niessen et al. [40] pointed out that the correct ordering of the $1\pi_u$ and $3\sigma_u$ MOs is obtained only with large basis sets which give results close to the Hartree–Fock limit. In the present case, the valence-only basis gives almost degenerate $1\pi_u$ and $3\sigma_u$ MOs, but the valence plus polarization basis gives more improved spacing. The SAC CI results compare reasonably well with the experimental values [46]. The correct ordering of the $^2\Pi_u(1\pi_u \to \infty)$ and $^2\Sigma_u(3\sigma_u \to \infty)$ states is obtained only when we use the valence plus polarization basis. This is the same tendency as the Green's function method as reported by von Niessen et al. [40]. Our results may not yet be stable to the basis set expansion. The notations "3-excited" and "3,4-excited" stand for calculations which include the unlinked terms $R^{(1)}S^{(2)}$ and $R^{(1)}S^{(2)} + R^{(2)}S^{(2)}$, respectively, where $R^{(1)}$ and $R^{(2)}$ denote one- and two-electron excitation operators, respectively, in eq. (12). Among the present SAC CI results, the "3,4-excited" calculations with the valence plus polarization basis (actually the most elaborate calculations) give best overall agreement with experiments. As shown by England et al. [12–15], the lowest ionization potential for the $^2\Pi_g(1\pi_g \to \infty)$ state appears difficult to calculate accurately with the CI method.

Table 9 shows the ionization potential of $N_2O$. Again the first four are outer-valence ionizations and the latter two inner-valence ionizations. The Koopmans values are always larger than the experimental values. Here, the orderings are correct in contrast to $CO_2$. As for the SAC CI results, the "3-excited" results compare better with experiment than the "3,4-excited" results, except for ionization from the $1\pi$ MO. Probably, the effect of polarization functions and the effect of "4-excited" configurations in the unlinked term may offset each other. The better result of the "3,4-excited" calculations for the ionization from the $1\pi$ MO seems to be due to a large mixing of shake-up configurations into this ionization as shown later in table 11. For the inner-valence ionizations, the main peaks observed at 35.5 eV and 39 eV [25] may be assigned to ionizations from the $5\sigma$ and $4\sigma$ MOs, respectively, though there is strong mixing of shake-up configurations as shown below.

Table 8
Ionization potential of $CO_2$ (eV)

| State | Orbital picture | Koopmans [a] | SAC CI [a,b] | | Exptl. [46] | CI England et al. [12–15] | CI Iwata [46] | Green's function [28,40] [c] |
|---|---|---|---|---|---|---|---|---|
| | | | 3-excited | 3,4-excited | | | | |
| $^2\Pi_g$ | $1\pi_g \to \infty$ | 14.77(14.71) | 13.97(13.61) | 13.42(13.11) | 13.78 | 13.07 | 13.01 | 13.66(13.49) |
| $^2\Pi_u$ | $1\pi_u \to \infty$ | 19.47(20.09) | 18.31(18.49) | 17.60(17.86) | 17.59 | 17.18 | 17.69 | 17.87(18.20) |
| $^2\Sigma_u$ | $3\sigma_u \to \infty$ | 20.17(20.10) | 18.40(17.91) | 17.69(17.33) | 18.08 | 18.38 | 17.84 | 18.30(18.12) |
| $^2\Sigma_g$ | $4\sigma_g \to \infty$ | 21.75(21.68) | 19.79(19.23) | 19.03(18.59) | 19.40 | 19.84 | 19.21 | 19.65(19.34) |
| $^2\Sigma_u$ | $2\sigma_u \to \infty$ | 40.25(41.31) | 36.41(38.11) | 35.61(36.77) | | – | – | 35.30 |
| $^2\Sigma_g$ | $3\sigma_g \to \infty$ | 41.76(42.74) | 38.12(39.15) | 36.52(36.91) | | – | – | 38.84 |

[a] Results of the valence plus polarization basis and valence-only basis are given without and with parentheses, respectively.
[b] SAC CI V result. The notation "3-excited" and "3,4-excited" stands for calculations including the unlinked terms, $R^{(1)}S^{(2)}$ and $R^{(1)}S^{(2)} + R^{(2)}S^{(2)}$, respectively, where $R^{(1)}$ and $R^{(2)}$ are one- and two-electron excitation operators, respectively. (See eq. (12).)
[c] The results of extended basis set and double-zeta basis set are given without and with parentheses, respectively.

Table 9
Ionization potential of NNO (eV)

| State | Orbital picture | Koopmans | SAC CI [a] | | Exptl. [46] | CI Iwata [46] | Green's function [28] |
|---|---|---|---|---|---|---|---|
| | | | 3-excited | 3,4-excited | | | |
| $^2\Pi$ | $2\pi \to \infty$ | 13.25 | 12.61 | 12.24 | 12.89 | 12.23 | 12.72 |
| $^2\Sigma$ | $7\sigma \to \infty$ | 18.94 | 16.47 | 15.59 | 16.38 | 16.01 | 16.38 |
| $^2\Pi$ | $1\pi \to \infty$ | 21.36 | 19.62 | 18.73 | 18.2 | 18.37 | 18.93 |
| $^2\Sigma$ | $6\sigma \to \infty$ | 22.36 | 19.96 | 19.40 | 20.11 | 19.96 | 20.53 |
| $^2\Sigma$ | $5\sigma \to \infty$ | 39.93 | – | 36.70 | 35.5 [b] | – | 34.83 |
| $^2\Sigma$ | $4\sigma \to \infty$ | 44.84 | – | 40.33 | 39 [b] | – | 38.63 |

[a] SAC CI V results with the valence-only basis.
[b] Ref. [25].

### 4.2. Inner-valence ionizations and satellite peaks

The inner-valence ionization spectra of $CO_2$ and $N_2O$ were observed by photoelectron spectroscopy [24–26] and by dipole (e–2e) spectroscopy [27,28]. Fig. 1 shows the photoelectron spectra of $CO_2$ (upper) and $N_2O$ (lower) observed by Allan et al. [24] and by Gelius [25], respectively. The broad and overlapping peaks suggest the existence of many satellite peaks in the inner-valence region. Theoretical studies were performed by Cederbaum et al. [29] and Domcke et al. [28] by the 2ph TDA Green function method. They attributed these satellite peaks as being due to strong correlation effects in the final ionized states. Arneberg et al. [47] also suggested the role of vibrational and vibronic effects.

As mentioned in section 2, the SAC CI theory involves a spirit of multi-reference CI through the unlinked terms of eq. (12). Though an ordinary excitation or ionization is essentially a one-electron process, inner-valence ionization includes simultaneous ionization–excitation (shake-up) processes which are two-electron processes. Therefore, in the spirit of multi-reference CI, we have to include up to two-electron excitation operators for the $R_K^\dagger$ operators in the unlinked terms of eq. (12), which result in three- and four-electron excited configurations. This calculation has been referred to as "3,4-excited" calculations in contrast to the "3-excited" calculations which includes only one-

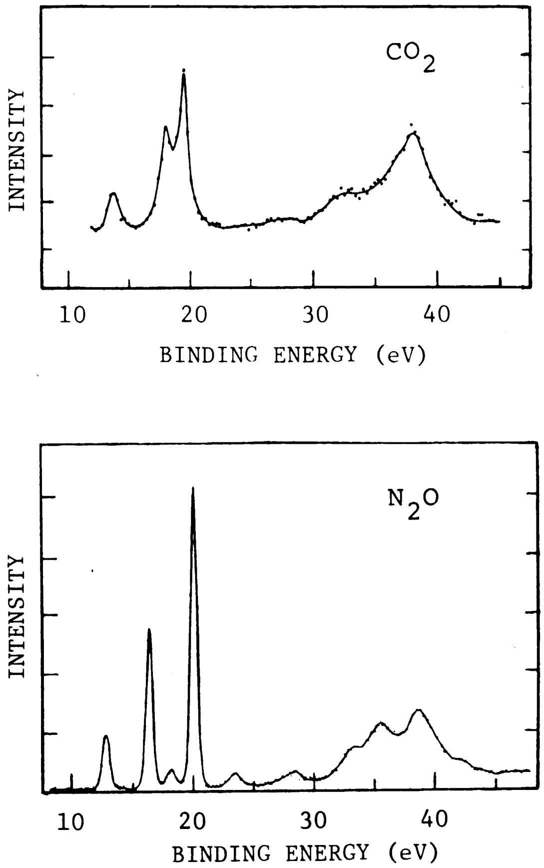


Fig. 1. Experimental photoelectron spectra of $CO_2$ (upper, from ref. [24]) and $N_2O$ (lower, from ref. [25]).

electron excitation operators for the $R_K^\dagger$ operators in the unlinked terms (which result in three-electron excited configurations). Here, we thus give the results of the "3,4-excited" calculations only.

Fig. 2 shows the calculated ionization spectra of $CO_2$ and $N_2O$ obtained commonly with the valence-only basis. The upper one is for $CO_2$ and the lower one for $N_2O$. Fig. 3 shows the ionization spectra of $CO_2$ calculated with the valence plus polarization basis. In tables 10 and 11, we have given more detailed results of the SAC CI calculations. Table 10 is for $CO_2$ obtained with the valence plus polarization basis and table 11 is for $N_2O$ obtained with the valence-only basis. The spectral intensity is assumed to be proportional to the transition monopole [47,48],

$$P_K = \sum_i |\langle \Psi_K^+ | a_i \Psi_g \rangle|^2 \approx \sum_i^{\text{occ}} |\langle \Psi_K^+ | a_i \Phi_0 \rangle^2, \tag{18}$$

where $\Psi_K^+$ is the wavefunction of the $K$th ionized state, $a_i$ annihilates an electron from the orbital $\phi_i$, and $\Phi_0$ is the Hartree–Fock reference configuration.

The present theoretical spectra shown in figs. 2 and 3 reproduce general features of the experimental photoelectron spectra shown in fig. 1. In the inner-valence region, 22–45 eV, the observed spectrum of $CO_2$ is composed of a single broad peak ranging from 30 to 43 eV with a flat shoulder in the 30–35 eV region. On the other hand, for $N_2O$, the main spectrum ranging from 30 to 43 eV is composed of several (at least four) split but overlapping peaks, and there are at least two distinct peaks in the 22–30 eV region. The theoretical spectra reproduce these general features and also the differences between the $CO_2$ and $N_2O$ spectra. The main peaks in the 30–43 eV region are considered to be due to the superposition of many peaks of inner-valence ionization and their satellites. The small peaks of $N_2O$ in the 22–30 eV region seem to be due to satellites of the ionizations from the $1\pi$, $6\sigma$ and $5\sigma$ orbitals.

Comparing fig. 3 with the upper half of fig. 2,

Table 10
Valence ionizations and satellite peaks of $CO_2$ calculated by the SAC CI theory [a)]

| Ionization energy (eV) | Main orbital | Intensity $P$ | Main configuration [b)] |
|---|---|---|---|
| 13.42 | $1\pi_g$ | 0.92 | $0.96(1\pi_g)^{-1}$ |
| 17.60 | $1\pi_u$ | 0.89 | $0.94(1\pi_u)^{-1}$ |
| 17.69 | $3\sigma_u$ | 0.90 | $0.95(3\sigma_u)^{-1}$ |
| 19.03 | $4\sigma_g$ | 0.89 | $0.94(4\sigma_g)^{-1}$ |
| 30.64 | $3\sigma_g$ | 0.02 | $0.85(1\pi_g)^{-2}(5\sigma_g)^1$ |
| 32.17 | $2\sigma_u$ | 0.03 | $0.40(1\pi_u)^{-1}(1\pi_g)^{-1}(5\sigma_g)^1$ |
| 32.66 | $1\pi_u$ | 0.03 | $0.75(1\pi_g)^{-2}(2\pi_u)^1$ |
| 35.58 | $1\pi_g$ | 0.02 | $0.68(1\pi_u)^{-1}(1\pi_g)^{-1}(2\pi_u)^1$ |
| 35.61 | $2\sigma_u$ | 0.67 | $0.82(2\sigma_u)^{-1}$ |
| 36.32 | $1\pi_u$ | 0.03 | $0.66(1\pi_g)^{-1}(3\sigma_u)^{-1}(5\sigma_g)^1$ |
| 36.52 | $3\sigma_g$ | 0.47 | $0.68(3\sigma_g)^{-1}$ |
| 36.96 | $2\sigma_u$ | 0.08 | $0.36(4\sigma_g)^{-1}(1\pi_g)^{-1}(2\pi_u)^1$ |
| 37.17 | $3\sigma_g$ | 0.18 | $0.67(3\sigma_u)^{-2}(5\sigma_g)^1$ |
| 39.74 | $3\sigma_g$ | 0.11 | $0.75(3\sigma_u)^{-2}(5\sigma_g)^1$ |
| 41.52 | $2\sigma_u$ | 0.08 | $0.44(1\pi_g)^{-1}(4\sigma_g)^{-1}(2\pi_u)^1$ |
| 41.97 | $3\sigma_g$ | 0.05 | $0.41(1\pi_u)^{-2}(5\sigma_g)^1$ |
| 42.14 | $3\sigma_g$ | 0.02 | $0.63(1\pi_u)^{-2}(5\sigma_g)^1$ |
| 42.64 | $3\sigma_g$ | 0.04 | $0.54(1\pi_g)^{-1}(3\sigma_u)^{-1}(3\pi_u)^1$ |
| 47.09 | $2\sigma_u$ | 0.02 | $0.41(3\sigma_u)^{-1}(1\pi_u)^{-1}(2\pi_u)^1$ |

[a)] From valence plus polarization basis. The Hartree–Fock orbital sequence is $(\text{core})^6(3\sigma_g)^2(2\sigma_u)^2(4\sigma_g)^2(3\sigma_u)^2(1\pi_u)^4(1\pi_g)^4(2\pi_u)^0(5\sigma_g)^0(4\sigma_u)^0(3\pi_u)^0\ldots$

[b)] The notation $(i)^{-1}$ and $(i)^{-1}(j)^{-1}(a)^1$ stands for the configurations $I_i|0\rangle$ and $I_iS_j^a|0\rangle$, respectively (see table 1).

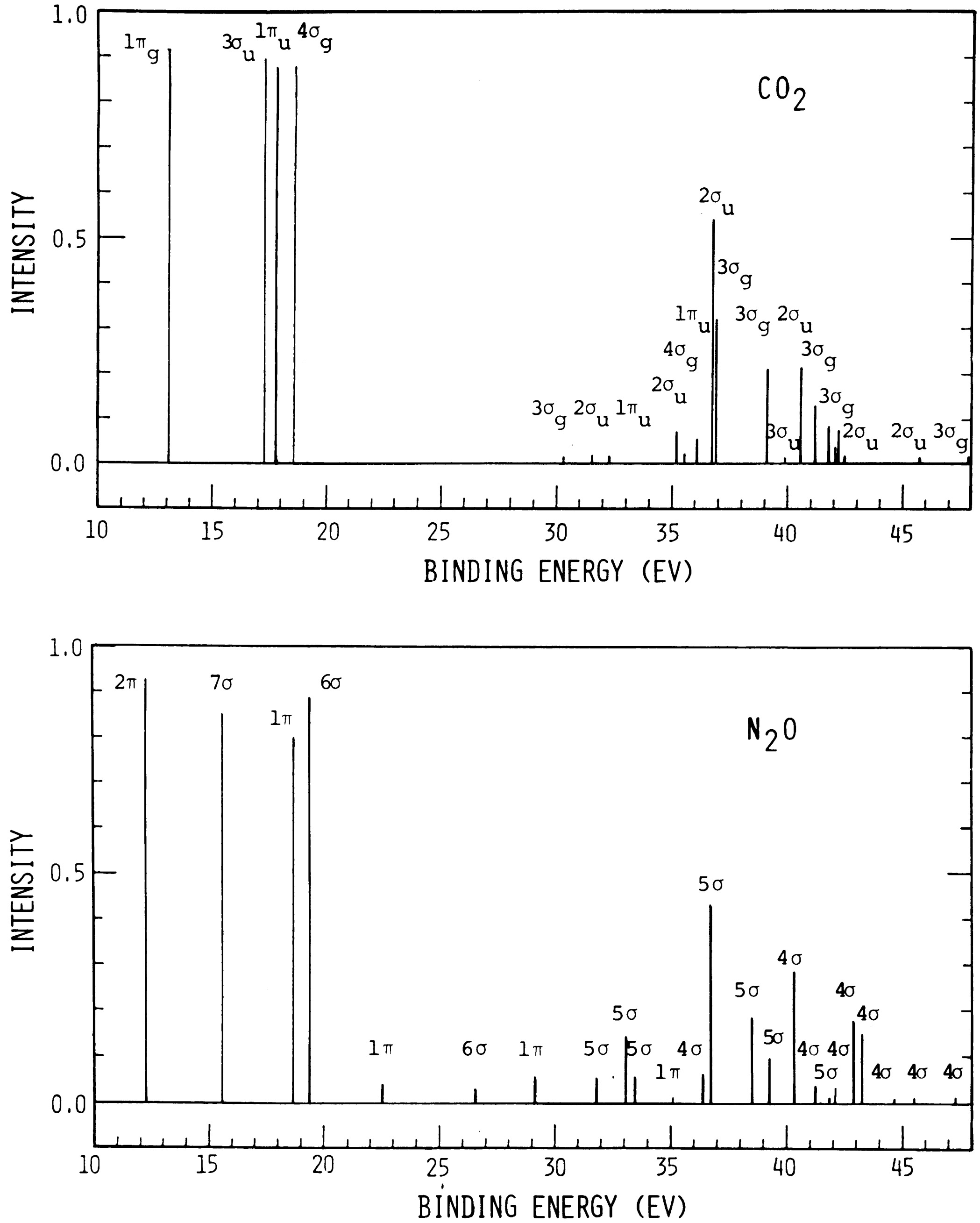


Fig. 2. Theoretical ionization spectra of $CO_2$ (upper) and $N_2O$ (lower) calculated by the SAC CI theory including three- and four-electron excitations in the unlinked terms. The basis sets are commonly the valence-only basis.

we see that the effect of d-polarization functions is to shift the group of peaks in the 30–43 eV region to the left by $\approx$ 1 eV. The main $2\sigma_u$ and $3\sigma_g$ peaks near 36 eV gain more intensity by the inclusion of d-orbitals and the satellites near 40 eV loose intensity, accordingly.

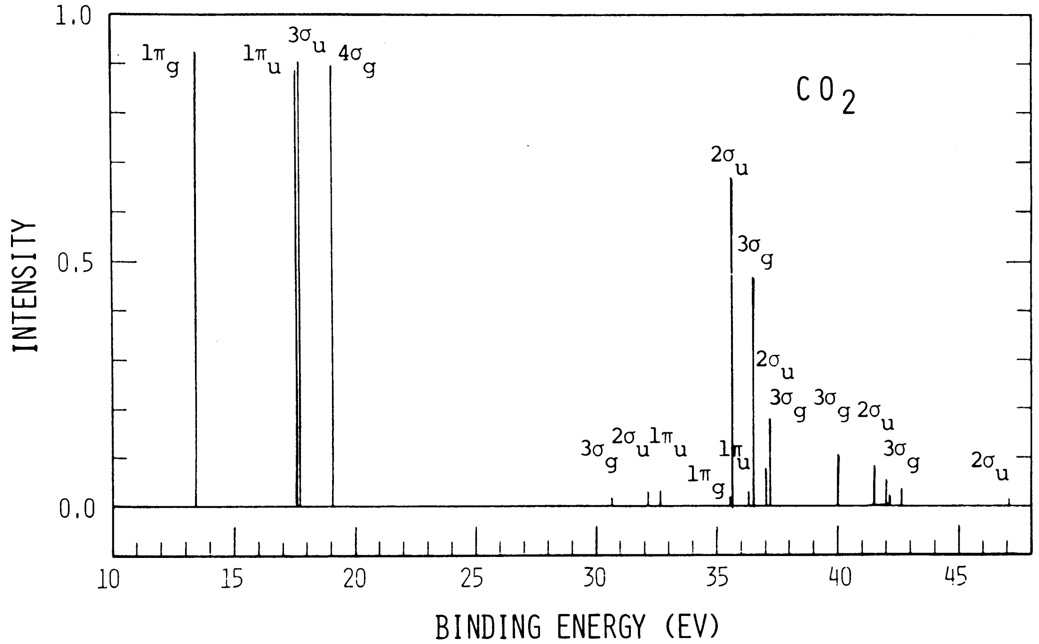


Fig. 3. Theoretical ionization spectra of $CO_2$ calculated by the SAC CI theory including three- and four-electron excitations in the unlinked terms. The basis is the valence plus polarization basis.

The detailed structures of the spectra of the inner-valence ionizations and their satellites are clarified only theoretically. Tables 10 and 11 give detailed information. For $CO_2$, the $2\sigma_u$ and $3\sigma_g$ peaks appear in the same overlapping energy regions. Namely, the $2\sigma_u$ peaks appear at 35.6 eV ($P = 0.67$), 37.0 eV ($P = 0.08$), and 41.5 eV ($P = 0.08$), and the $3\sigma_g$ peaks appear at 36.5 eV ($P = 0.47$), 37.2 eV ($P = 0.18$), 39.7 eV ($P = 0.11$), and 42.0 eV ($P = 0.05$). On the other hand, for $N_2O$, the $5\sigma$ and $4\sigma$ peaks appear in separate energy regions. Namely, the $5\sigma$ peaks appear at 33.1 eV ($P = 0.15$), 36.7 eV ($P = 0.43$), and 38.5 eV ($P = 0.19$), but the $4\sigma$ peaks appear at higher energies, 39.3 eV ($P = 0.10$), 40.3 eV ($P = 0.29$), 42.9 eV ($P = 0.18$), and 43.3 eV ($P = 0.15$). This seems to be the main reason of the difference in the observed spectra in the 33–43 eV region, i.e. a single broad peak for $CO_2$ and split overlapping peaks for $N_2O$. (This feature is already seen in the Hartree–Fock orbitals. Namely, the orbital energies of the $2\sigma_u$ and $3\sigma_g$ MOs of $CO_2$ are $-40.25$ and $-41.76$ eV, the difference being only 1.51 eV, whilst those of the $5\sigma$ and $4\sigma$ MOs of $N_2O$ are $-39.93$ and $-44.84$ eV, which differ by as much as 4.91 eV.) Thus, for $N_2O$ we can assign the three strong and distinct peaks observed at 33, 36 and 39 eV as ionizations from the $5\sigma$ (33.1 eV), $5\sigma$ (36.7 eV), and $4\sigma$ (39.3 and 40.3 eV) MOs, respectively. The shoulder at 42.5 eV is assigned to the $4\sigma$ MO (42.9 eV). For $CO_2$, however, the excitations from the $2\sigma_u$ and $3\sigma_g$ MOs overlap more closely so that distinct assignments are impossible. Anyway, since the orbital picture is broken down almost completely for these ionized states, these assignments to the MOs are almost meaningless, and we have better use the assignments as given in tables 10 and 11.

As origins of the shake-up configurations in the satellite peaks, the excitations from the $4\sigma_g$, $3\sigma_u$, $1\pi_u$, and $1\pi_g$ MOs to the $5\sigma_g$, $2\pi_u$, and $3\pi_u$ MOs are important for $CO_2$ and the excitations from the $6\sigma$, $1\pi$, $2\pi$, and $7\sigma$ MOs to the $8\sigma$ and $3\pi$ MOs are important for $N_2O$. These occupied orbitals are bonding MOs between neighboring atoms or non-bonding MOs and the unoccupied MOs are

Table 11
Valence ionizations and satellite peaks of NNO calculated by the SAC CI theory [a)]

| Ionization energy (eV) | Main orbital [b)] | Intensity $P$ | Main configuration [c)] |
|---|---|---|---|
| 12.24 | $2\pi$ | 0.93 | $0.96(2\pi)^{-1}$ |
| 15.59 | $7\sigma$ | 0.85 | $0.91(7\sigma)^{-1}$ |
| 18.73 | $1\pi$ | 0.80 | $0.89(1\pi)^{-1}-0.41(2\pi)^{-2}(3\pi)^{1}$ |
| 19.40 | $6\sigma$ | 0.89 | $0.93(6\sigma)^{-1}$ |
| 22.50 | $1\pi$ | 0.04 | $0.83(2\pi)^{-2}(3\pi)^{1}$ |
| 26.50 | $6\sigma(5\sigma)$ | 0.03 | $0.74(2\pi)^{-1}(7\sigma)^{-1}(3\pi)^{1}$ |
| 29.14 | $1\pi$ | 0.06 | $0.63(2\pi)^{-2}(3\pi)^{1}$ |
| 31.81 | $5\sigma(6\sigma)$ | 0.06 | $0.37(7\sigma)^{-1}(2\pi)^{-1}(3\pi)^{1}$ |
| 33.06 | $5\sigma$ | 0.15 | $0.37(5\sigma)^{-1}+0.36(1\pi)^{-1}(2\pi)^{-1}(8\sigma)^{1}$ |
| 33.43 | $5\sigma(4\sigma)$ | 0.06 | $0.43(1\pi)^{-1}(7\sigma)^{-1}(3\pi)^{1}$ |
| 35.08 | $1\pi$ | 0.01 | $0.55(2\pi)^{-1}(1\pi)^{-1}(3\pi)^{1}$ |
| 36.43 | $4\sigma(5\sigma)$ | 0.06 | $0.71(6\sigma)^{-1}(7\sigma)^{-1}(8\sigma)^{1}$ |
| 36.70 | $5\sigma$ | 0.43 | $0.63(5\sigma)^{-1}$ |
| 38.50 | $5\sigma$ | 0.19 | $0.53(2\pi)^{-1}(1\pi)^{-1}(8\sigma)^{1}+0.49(1\pi)^{-1}(2\pi)^{-1}(8\sigma)^{1}-0.43(5\sigma)^{-1}$ |
| 39.27 | $4\sigma$ | 0.10 | $0.60(7\sigma)^{-1}(6\sigma)^{-1}(8\sigma)^{1}$ |
| 40.33 | $4\sigma$ | 0.29 | $0.53(4\sigma)^{-1}+0.35(7\sigma)^{-1}(6\sigma)^{-1}(8\sigma)^{1}$ |
| 41.25 | $4\sigma(5\sigma)$ | 0.03 | $0.49(2\pi)^{-1}(7\sigma)^{-1}(4\pi)^{1}$ |
| 41.85 | $5\sigma(6\sigma)$ | 0.01 | $0.74(2\pi)^{-2}(10\sigma)^{1}$ |
| 42.12 | $4\sigma(6\sigma)$ | 0.04 | $0.48(7\sigma)^{-1}(2\pi)^{-1}(4\pi)^{1}$ |
| 42.88 | $4\sigma$ | 0.18 | $0.46(1\pi)^{-1}(6\sigma)^{-1}(3\pi)^{1}+0.41(4\sigma)^{-1}$ |
| 43.25 | $4\sigma(5\sigma)$ | 0.15 | $0.44(6\sigma)^{-1}(2\pi)^{-1}(3\pi)^{1}+0.32(4\sigma)^{-1}$ |
| 44.64 | $4\sigma(5\sigma)$ | 0.01 | $0.44(1\pi)^{-1}(2\pi)^{-1}(9\sigma)^{1}$ |
| 45.53 | $4\sigma$ | 0.01 | $0.54(2\pi)^{-2}(11\sigma)^{1}$ |
| 47.36 | $4\sigma$ | 0.01 | $0.61(1\pi)^{-2}(8\sigma)^{1}$ |

[a)] From valence-only basis. The orbital sequence is $(\text{core})^6(4\sigma)^2(5\sigma)^2(6\sigma)^2(1\pi)^4(7\sigma)^2(2\pi)^4(3\pi)^0(8\sigma)^0(9\sigma)^0(4\pi)^0(10\sigma)^0(5\pi)^0(11\sigma)^0(12\sigma)^0\ldots$.
[b)] In parentheses, the secondary, but close to main, orbital is given.
[c)] The notation $(i)^{-1}$ and $(i)^{-1}(j)^{-1}(a)^{1}$ stands for the configurations $I_i|0\rangle$ and $I_iS_j^a|0\rangle$, respectively (see table 1).

antibonding MOs, so that in the inner-valence ionized states and their satellite states, considerable elongations in bond length should occur. This effect should also be a reason of the broadness of the peaks. (This effect tends to shift the overall shape of the spectrum to the lower-energy region.) Further, we see from fig. 2 that many weak peaks are embedded between the relatively strong peaks. This is also an origin of the broadness of the peaks in the inner-valence region.

## 5. Summary and conclusion

In this paper, we have studied the valence and Rydberg excitations, ionizations, and inner-valence ionizations and their satellites for $CO_2$ and $N_2O$, an isoelectronic pair of molecules. These various excited states were studied by the SAC CI theory based on the SAC wavefunction for the ground state. For $CO_2$, some controversial situations were there in the assignments of the electronic spectra. Our results are relatively close to the results of England and Ermler [12]. Based on the present results, we have given a systematic assignment of the observed spectra. For $N_2O$, a similar situation exists, though the studies were more limited than for $CO_2$. The present study is most comprehensive and accurate. For the valence excitations of $CO_2$ and $N_2O$, a change in geometry, mainly in the valence angle [21], seems to make the spectra complex. the Rydberg excitations of $CO_2$

and $N_2O$ are rather simple and easily assigned, except for the $^{1,3}\Pi_g(R)$ states of $CO_2$, because the change in geometry due to excitation should be small for Rydberg excitations [21]. The $^{1,3}\Pi_g(R)$ states of $CO_2$ are lower than the valence excited states, so that they mix strongly with the valence excited states and suffer an avoided crossing, when the molecule is bent in the excited states [12]. For $N_2O$, the Rydberg excited states are well above the valence excited states, so that such a complexity does not occur. The assignments of the spectra were therefore simpler for $N_2O$ than for $CO_2$.

The SAC CI theory has also given satisfactory results for the ionization spectra of $CO_2$ and $N_2O$ in both valence and inner-valence regions. The broad and overlapping features of the spectra of the inner-valence ionizations are explained as being due to strong final correlation effects, i.e. the existence of many shake-up states mixing with the single-ionization states. This supports the result obtained by Domcke et al. [28] by the 2ph TDA method. The similarities and the differences in the photoelectron spectra of $CO_2$ and $N_2O$ have found their own theoretical origins. We note that an ordinary multi-reference CI method is very difficult to be applied to the study of inner-valence ionizations, because many eigenvalues and eigenvectors of matrices of large dimensions should be solved [47]. The SAC CI theory can be applied easily to this study because it is more rapidly convergent than ordinary CI methods.

Finally, we note that in all calculations of the ground state, valence and Rydberg excited states, and outer- and inner-valence ionizations, we have used commonly the same reference orbitals, i.e. the closed-shell RHF orbitals of the neutral ground state. This is important and useful for theoretical and computational consistency and simplicity.

## Acknowledgement

The calculations were carried out with the M-200 computers at the Data Processing Center of Kyoto University and at the Institute for Molecular Science. The author thanks both of these computer centers for giving him computer time. Part of this study was also supported by the Japan Sociaty for the Promotion of Science.

## References

[1] S.D. Peyerimhoff and R.J. Buenker, Advan. Quantum Chem. 9 (1975) 69;
R.J. Buenker, S.D. Peyerimhoff and W. Butscher, Mol. Phys. 35 (1978) 771;
B. Liu and M. Yoshimine, J. Chem. Phys. 74 (1981) 612.
[2] G. Das, J. Chem. Phys. 58 (1973) 5104;
F. Grein and A. Banerjee, Intern. J. Quantum Chem. S9, (1975) 147;
K. Ruedenberg, L.M. Cheung and S.T. Elbert, Intern. J. Quantum Chem. 16 (1979) 1069.
[3] D. Mukherjee, R.K. Moitra and A. Mukhopadhyay, Mol. Phys. 30 (1975) 1861; 33 (1977) 955;
A. Mukhopadhyay, R.K. Moitra, and D. Mukherjee, J. Phys. B12 (1979) 1;
J. Paldus, J. Čižek, M. Saute and A. Laforgue, Phys. Rev. 17 (1978) 805;
M. Saute, J. Paldus and J. Čižek, Intern. J. Quantum Chem. 15 (1979) 463;
I. Lindgren, Intern. J. Quantum Chem. S12 (1978) 33;
I. Ohmine, M. Karplus and K. Schulten, J. Chem. Phys. 68 (1978) 2298;
I. Ohmine, Chem. Phys. Letters 72 (1980) 53.
[4] H. Nakatsuji and K. Hirao, J. Chem. Phys. 68 (1978) 2053.
[5] K. Hirao and H. Nakatsuji, Chem. Phys. Letters 79 (1981) 292.
[6] H. Nakatsuji, Chem. Phys. Letters 59 (1978) 362.
[7] H. Nakatsuji, Chem. Phys. Letters 67 (1979) 329.
[8] H. Nakatsuji, Chem. Phys. Letters 67 (1979) 334;
H. Nakatsuji and K. Hirao, Intern. J. Quantum Chem. 20 (1981) 1301;
H. Nakatsuji, K. Ohta and K. Hirao, J. Chem. Phys. 75 (1981) 2952.
[9] H. Nakatsuji and T. Yonezawa, Chem. Phys. Letters 87 (1982) 426.
[10] H. Nakatsuji and K. Hirao, Chem. Phys. Letters 47 (1977) 569; J. Chem. Phys. 68 (1978) 4279;
K. Hirao and H. Nakatsuji, J. Chem. Phys. 69 (1978) 4548;
K. Ohta, H. Nakatsuji, K. Hirao and T. Yonezawa, J. Chem. Phys. 73 (1980) 1770.
[11] H. Nakatsuji, K. Ohta and T. Yonezawa, J. Phys. Chem. (1983), to be published.
[12] W.B. England and W.C. Ermler, J. Chem. Phys. 70 (1979) 1711.
[13] W.B. England, W.C. Ermler and A.C. Wahl, J. Chem. Phys. 66 (1977) 2336.
[14] W.B. England, B.J. Rosenberg, P.J. Fortune and A.C. Wahl, J. Chem. Phys. 65 (1976) 684.
[15] W.B. England and W.C. Ermler, J. Mol. Spectry. 85 (1981) 341.
[16] N.W. Winter, C.F. Bender and W.A. Goddard III, Chem. Phys. Letters 20 (1973) 489.
[17] J.W. Rabalais, J. McDonald, V. Scherr and S.P. McGlynn, Chem. Rev. 71 (1971) 73.
[18] M.J. Hubin-Franskin and J.E. Collin, Bull. Soc. Roy. Sci. Liege 40 (1971) 361.

[19] R.I. Hall, A. Chutjian and S. Trajmar, J. Phys. B6 (1973) L264.
[20] C.W. McCurdy Jr. and V. McKoy, J. Chem. Phys. 61 (1974) 2820;
W. England, D. Yeager and A.C. Wahl, J. Chem. Phys. 66 (1977) 2344.
[21] H. Nakatsuji, J. Am. Chem. Soc. 95 (1973) 345, 354;
H. Nakatsuji and T. Koga, in: The force concept in chemistry, ed. B.M. Deb (Van Nostrand, Princeton, 1981) ch. 3, pp. 137–217.
[22] R.I. Hall, A. Chutjian and S. Trajmar, J. Phys. B6 (1973) L365.
[23] A. Chutjian and G.A. Segal, J. Chem. Phys. 57 (1972) 3069.
[24] C.J. Allan, U. Gelius, D.A. Allison, G. Johansson, H. Siegbahn and K. Siegbahn, J. Electron Spectry. 1 (1972), 131.
[25] U. Gelius, J. Electron Spectry. 5 (1974) 985.
[26] A.W. Potts and T.A. Williams, J. Electron Spectry. 3 (1974) 3.
[27] C.E. Brion and K.H. Tan, Chem. Phys. 34 (1978) 141.
[28] W. Domcke, L.S. Cederbaum, J. Schirmer, W. von Niessen, C.E. Brion and K.H. Tan, Chem. Phys. 40 (1979) 171.
[29] L.S. Cederbaum, J. Schirmer, W. Domcke and W. von Niessen, J. Phys. B10 (1977) L549.
[30] J. Schirmer and L.S. Cederbaum, J. Phys. B11 (1978) 1889.
[31] D.J. Thouless, Nucl. Phys. 21 (1960) 225; 22 (1961) 78;
F.E. Harris, Intern. J. Quantum Chem. S11 (1977) 403.
[32] O. Sinanoğlu, Advan. Chem. Phys. 6 (1964) 315;
J. Čížek, J. Chem. Phys. 45 (1966) 4256; Advan. Chem. Phys. 14 (1969) 35;
J. Čížek and J. Paldus, Intern. J. Quantum Chem. 5 (1971) 359;
J. Paldus, J. Čížek and I. Shavitt, Phys. Rev. A5 (1972) 50;
W. Kutzelnigg, in: Modern theoretical chemistry, Vol. 3, ed. H.F. Schaefer III (Plenum Press, New York, 1977) p. 129;
R.J. Bartlett and G.D. Purvis III, Physica Scripta 21 (1980) 255.
[33] H. Nakatsuji, Program System for SAC and SAC-CI Calculations, unpublished.
[34] A. Messiah, Mécanique quantique (Dunod, Paris, 1959).
[35] E.R. Davidson, J. Comput. Phys. 17 (1975) 87.
[36] K. Hirao and H. Nakatsuji, J. Comput. Phys. 45 (1982) 246;
S. Rettrup, J. Comput. Phys. 45 (1982) 100.
[37] I. Shavitt, in: Modern theoretical chemistry, vol. 3, ed. H.F. Schaefer III (Plenum Press, New York, 1977) p. 189.
[38] S. Huzinaga, J. Chem. Phys. 42 (1965) 1293.
[39] T.H. Dunning Jr. and P.J. Hay, in: Modern theoretical chemistry, Vol. 3, ed. H.F. Schaefer III (Plenum Press, New York, 1977) p. 1.
[40] W. von Niessen, G.H.F. Diercksen and L.S. Cederbaum, J. Chem. Phys. 67 (1977) 4124.
[41] G. Herzberg, Molecular spectra and molecular structure, Vol. 3. Electronic spectra and electronic structure of polyatomic molecules (Van Nostrand, Princeton, 1965).
[42] R.S. Mulliken, Accounts Chem. Res. 9 (1976) 7.
[43] S.D. Peyerimhoff and R.J. Buenker, J. Chem. Phys. 49 (1968) 2473.
[44] N.W. Winter, Chem. Phys. Letters 33 (1975) 300.
[45] A.D. McLean and M. Yoshimine, J. Chem. Phys. 45 (1966) 3676.
[46] K. Kimura, S. Katsumata, Y. Achiba, T. Yamazaki and S. Iwata, Handbook of HeI photoelectron spectra of fundamental organic molecules (Halstead Press, New York, 1981).
[47] R. Arneberg, J. Müller and R. Manne, Chem. Phys. 64 (1982) 249.
[48] R.L. Martin and D.A. Shirley, J. Chem. Phys. 64 (1976) 3685.